Redlining and Urban Heat Islands: An analysis of historic housing discrimination and heat exposure

By
Hannah Mosiniak

A thesis submitted
in partial fulfillment of the requirements
for the degree of
Master of Science
(Environment and Sustainability)
in the University of Michigan
December 2021

Thesis Committee:
Professor Derek Van Berkel, Chair
Shannon Brines

Abstract

Urban heat islands (UHI) are a phenomenon observed in built environments due to differences in terrestrial albedo that result in higher temperatures in urban areas. Variations in both environmental factors and physical infrastructure cause a wide range in temperature among neighborhoods within the same city. In the 1930's, the Home Owners' Loan Corporation (HOLC) used risk assessment maps (now commonly referred to as redlining maps) to further reinforce racist housing and lending policies that were commonplace in that era. This study assesses the environmental legacy of these policies on current heat islands. The analysis is based on land surface temperature (LST) estimates derived from Landsat 8 (OLI/TIRS) imagery and calculated using open-source code in Google Earth Engine. Differences in LST are calculated for 8,865 unique HOLC neighborhoods for 202 cities across the United States. A linear mixed effects model is used to analyze if urban areas have varying temperatures in the present day based on their historic HOLC ranking (scale of A-D, where neighborhoods ranked A were typically limited to upper-class white residents, and neighborhoods ranked D were typically composed of Black residents regardless of class or income). The model found that all grades were significantly different from each other ($p<0.001$), with zones ranked D an estimated 2.3°C hotter than zones ranked A. These findings indicate that despite the cessation of overt race-based housing policies, the effects of such policies are socially and environmentally measurable in the present day.

Acknowledgements

This thesis would not have been possible without the support and inspiration from advisors, instructors, colleagues, family, and friends.

I would first like to thank my advisor and chair of this thesis, Dr. Derek Van Berkel. You've had more faith in me than I've had myself, and I cannot fully express my gratitude for your feedback, support, and care.

Thank you also to my instructor and second reader on this thesis, Shannon Brines, for your excellent classes, insightful feedback, and encouragement. Thank you to my instructors, Dr. Paige Fischer and Dr. Drew Gronewald, whose courses helped shape the ideas for this thesis. Thank you, Dr. Meha Jain, for supporting my change in thesis topic, even if it meant leaving her incredible lab. Lastly, thank you, Dr. Bilal Butt, for a single email that made me reevaluate my entire thesis topic and change it for the better. I am particularly grateful for the assistance from Kim Elliott and Jennifer Taylor who helped me plan for academic success.

I would also like to thank my wonderful classmates at SEAS. Cara Thuringer, Roshan, Krishnan, Shannon Blair, and Shannon Lloyd constantly inspired me to work harder and read more to keep up with them. Thank you, Rae Green, Colin Welk, and Julie Dellick, for providing so much support, inspiration, and hijinks.

This project has evolved over several years but was originally inspired by Meg Fredericks' (and team) NASA DEVELOP Project. Thank you for loving Landsat as much as I do. And thank you to all my inspirational coworkers at DEVELOP, including Patrick Frier, Max Stewart, Cecil Byles, Will Crowley, Jared Belvin, Carter Grimm, and Rachel Green.

I would also like to thank my former coworker Rob Anderson who influenced me to push the limits of my GIS knowledge, encouraged me to go to graduate school, and kept me mostly sane. Our long discussions of philosophy, geography, and everything in-between were invaluable. Thank you also to Maddie McNerthney

Thank you to my mother, siblings, nieces and nephews, stepmother, grandparents, and cousins for being so supportive. Thank you as well to Jad Salem whose support and friendship have buoyed me through three degrees. Lastly, thank you to my partner for feedback, intellectual discussions, code assistance, and unconditional support.

Table of Contents

Table of Contents

Introduction

Heat waves are especially dangerous in urban areas due to the urban heat island (UHI) effect. This phenomenon describes the notable variance in temperature between rural and urban areas due to differences in terrestrial albedo (Susca et al., 2011). Cities often have a high percentage of impervious surfaces (such as concrete and asphalt) that absorb and retain heat while rural areas have more vegetation that regulates and dissipates heat more quickly. Because cities have a higher population density, more people are subject to the effects of UHI, the impact of which will become more extreme as the global surface temperature continues to increase (Hansen, 2010). This is likely to impact residential populations differently due to legacies of variation in the built environment, access to greenspace, and difference in vulnerability to heat.

Some segments of the population will more acutely experience the negative impacts of increased heat. Age (both extremes of young and old) as well as preexisting health conditions play a large role in an individual’s vulnerability to heat (Benmarhnia et al., 2015; Sheffield et al., 2018; Stafoggi et al., 2006). Additionally, race and socioeconomic status play a role in one’s risk of heat related illness (Harlan et al., 2006). According to Harlan et al., cities contain microclimates caused by density of built environments and amount of vegetation, and the hotter microclimates tend to have higher rates of poverty and fewer resources to manage heat exposure. The correlation between hotter sections of a city and higher poverty can be traced back to the practice of redlining. Towards the end of the Great Depression, Roosevelt’s New Deal instituted the Home Owners’ Loan Corporation (HOLC) with the stated intention to help struggling homeowners keep their property through financing mortgages. The HOLC drew “Residential Security” maps that sectioned the cities into four distinct rankings: Best (A), Still Desirable (B), Definitely Declining (C), and Hazardous (D). These ranks were based on multiple factors including class, socioeconomic status, and race; most notably, neighborhoods with Black residents were almost always given a rank of D, regardless of any other attributes (Rothstein, 2018). Non-white homebuyers looking to take out loans to purchase in areas ranked A or B were denied loans. As a result, areas ranked C and D experienced higher rates of segregation (Hillier, 2003).

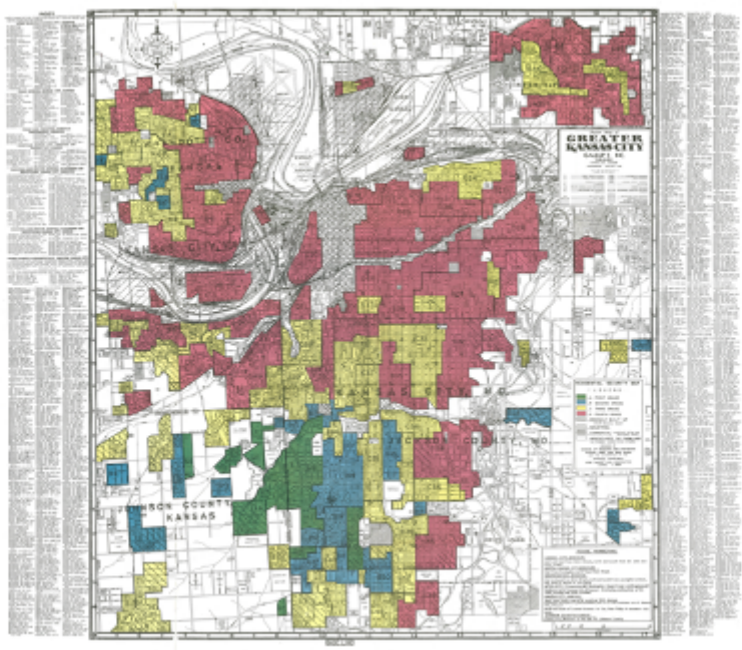

Figure 1. Example of an HOLC map showing redlined districts in the Greater Kansas City area. The term “redlining” comes from the reddish hue used to denote the lowest ranked zones.

While the practice of actively zoning residential areas by race is federally illegal now, the pattern created by redlining is still evident in cities across the U.S. even today. Table 1 is reproduced from a 2018 study by the NCRC (National Community Reinvestment Coalition). It depicts the percent of white and minority residents in each class of the redlined districts and shows that despite the cessation of overt race-based housing policies, a majority of the population in zones that were historically rank A are white (Mitchell et al., 2018). Urban areas still experience the extant impact of segregation decades later.

	White	Minority
A Best	85.82%	14.18%
B Desirable	71.57%	28.43%
C Declining	54.91%	45.09%
D Hazardous	35.16%	63.84%

Table 1. Percent white and percent minority by redline classifications (data: 2016 FFIEC Census- and ACS). Table originally published in an NCRC report by Mitchell et al.

The relationship between impervious surfaces and redlined districts is not by chance. A year after the creation of the HOLC, the Federal Housing Authority (FHA) was established, and the following year, they instituted the *Underwriting Manual*, a guidebook on policy that explicitly required racial segregation (Rothstein, 2018). Section 229 of 1936 version of the document states (FHA, 1936):

> Natural or artificially established barriers will prove effective in protecting a neighborhood and the locations within it from adverse influences. Usually the protection … include[s] prevention of the infiltration of business and industrial uses, lower-class occupancy, and inharmonious racial groups… A high-speed traffic artery or a wide street parkway may prevent the expansion of inharmonious uses to a location... On the other hand, when a high-speed traffic artery passes directly through a desirable neighborhood area with similar development on each side of the artery, instead of offering a protection the noise and danger [are] an adverse influence.

This section of the manual demonstrates that not only was segregation of "inharmonious racial groups" a key goal of the FHA, but the presence of highway infrastructure was also a key factor in determining the value and desirability of an area, whereas the presence of a highway detracted from the value of a community. Despite the end of overt racial segregation, the use of built infrastructure to divide, displace, and sometimes destroy communities continues garner federal approval into the present day (Bullard, 2004). The unintended consequence of this practice has led to an oversaturation of impervious surfaces in C and D ranked neighborhoods, which creates zones prone to the UHI effect.

Methodology

This study poses the following question: Do urban areas have varying temperatures in the present day based on their historic HOLC ranking? To test the impact of the legacy of racist housing policies on present-day heat exposure, this study fit a mixed effect multilevel model with LST as the dependent variable and tested it against environmental factors that might impact temperature variation within cities. These factors included elevation, latitude, longitude, and NDVI. Because the LST values used in this study are derived from NDVI, there was high multicollinearity, and NDVI was removed from the analysis.

Study Area

The study area comprises all cities in the United States that experienced redlining through the HOLC. Notably, Washington D.C. experienced a similar implementation of redlining, however it was not through the HOLC and used a different ranked scale, and therefore, D.C. was not included in the *Mapping Inequality* dataset. An ANOVA was conducted to determine if the hypothesis of this paper held true for D.C., and the results are included in Appendix Figure I. The analysis in this paper does not include D.C. due to the different methods for classifications.

All other U.S. cities that experienced redlining are included in this dataset. A full list is available in the appendix.

Redlined Cities Across the United States

Figure 2: All U.S. cities that have HOLC redlining maps

Data Acquisition and processing

HOLC Redlining Grades - Independent Variable

HOLC redlined zones for the contiguous United States were acquired through the University of Richmond's Digital Scholarship Lab’s *Mapping Inequality* project website. The research team that created *Mapping Inequality* digitized the original HOLC maps from the National Archives’ *Residential Security Maps* collection. This distinguishes HOLC zones for 202 cities and includes a measure of grade and area descriptions for each location. Nine data points were removed due to incomplete records (no ranking listed).

Digital Elevation Model (DEM) - Independent Variable

A 30m (one arc-second) digital elevation model was obtained from the National Elevation Dataset (NED) 30 through the United States Geological Survey (USGS). The DEM was clipped to the HOLC shapefile, and the average elevation per unique HOLC zone calculated in R.

Latitude and longitude were also calculated to control for differences in climate conditions across the U.S. as higher latitudes experience less extreme heat in the United States.

Land Surface Temperature (LST) - Dependent Variable

LST data were acquired through Google Earth Engine (GEE) using open-source code developed by Ermida et al. to extract LST estimates from Landsat satellites. The satellite used for this project was Landsat 8 Operational Land Imager/Thermal Infrared Sensor (OLI/TIRS) Collection 1, Tier 1, and the imagery was limited to scenes captured between June 1 – August 31, 2018. Based on a sample analysis of NOAA temperature data in 2018, these months were consistently the hottest and had fewer fluctuations in temperature, unlike late spring and early autumn months. Landsat 8 has a temporal resolution of 16 days, meaning there are at most 5 scenes available for any given city. Because most cities were small in area compared to a full Landsat scene, all scenes were acquired regardless of percentage of cloud cover then cloud masked. The selected scenes were then clipped to cities in the HOLC shapefile and averaged (in cases with multiple scenes or overlapping scenes).

LST was then calculated using the open-source Ermida et al. code in GEE. Due to calibration issues with band 11 of the Landsat 8 TIRS sensor, a split-window algorithm produced LST values with lower accuracy, and therefore the code from Ermida et al. uses a Statistical Mono-Window (SMW) algorithm that was developed by the Climate Monitoring Satellite Application Facility (CM-SAF). Accuracy tests performed by Ermida et al. indicate that the values are accurate within 0.5° K with overall RMSE values of approximately 2° K.

The LST calculations for Fort Worth and Dallas, TX were recalculated to include only one scene (LC08_L1TP_027037_20210821_20210827_01_T1) due to an error with the cloud mask that resulted in negative LST values when using the mean pixel value. No other such errors were found in other scenes.

The LST imagery was then exported from GEE as TIFF files and loaded into R Studio. Using the packages raster, sf, and exactextractr, the average temperature (in °K) for each redlined zone of the HOLC shapefile was calculated (Hijmans 2015; Pebesma 2018; Baston 2021). The exact_extract function of the exactextractr package calculates the zonal statistics (for this study, the mean LST value) of the polygons. The function efficiently handles grid cells that overlap the boundaries of a polygon, and, when calculating the mean, weights the fraction of a cell that overlaps with the polygon. The average temperature was then converted from °K to both °C and °F for easier visualization.

Data Analysis

The HOLC, LST, and DEM data sets were joined in R and a linear mixed effects model was run. A mixed effects model was necessary for this dataset due to the differing climates of cities across the contiguous United States. For example, the average air temperature of Dallas, TX on August 1st is 35.6°C[1], while in Binghamton, NY, the average temperature for the same date is 26.7°C[2]. It is worth noting that official temperature data supplied by NOAA are recorded almost exclusively at airports that are typically on the periphery of a city. As a result, these values do not reflect the ambient temperature within a city.

Multiple zones exist within each city, which creates a hierarchical structure within the dataset. To analyze the data without violating independence of our samples, the model must account for the variability between cities. The linear mixed effect model does this by assuming a different intercept for each city. Table 2 shows different constructions of the model that were considered for this analysis. As Model 5 shows, when city was not included as a random effect, the adjusted value was 40%, considerably lower than the models that did control for city. In addition to the inter-city differences in climate, there are intra-city differences in microclimates as well, usually due to features such as elevation, vegetation, and impervious surfaces (Harlen et al., 2006). This paper intends to show that these environmental differences that create microclimates can be modeled using the HOLC zones.

Model #	Variables	Adjusted R^2	Significant Variables ($p \leq 0.5$)
Model 1	Grade + City	0.767	All grades
Model 2*	Grade + DEM + City	0.849	All grades and DEM
Model 3	Grade + DSM + City	0.861	All grades and DSM
Model 4	Grade + DEM + lat + long + City	0.846	All grades and all variables
Model 5	Grade + DEM + lat + long	0.408	All grades and all variables

Table 2: Variations of the model considered for this analysis. Model 2 was chosen for analysis in this paper.

Variations of this model were run to determine best fit. Table 2 shows a sample of five of the models tested. Ultimately, model 2 was chosen to continue the analysis. Model 1 used only the HOLC grades and controlled for city, while it gave promising results, it did not account for enough of the variation within a city. Model 3 is identical to model 2 except the elevation data was from a digital surface model (DSM) rather than the DEM. DSMs tell the elevation of objects on the surface such as buildings or trees, while a DEM estimates the actual surface of the earth. Future work with this data could parse the land cover of the DSM to indicate what higher elevations are structures or tree canopy. This would add a layer of depth to the model that may increase the explanatory power by differentiating between built structures and vegetation. Model 4 included the DEM as well as latitude and longitude. No city in the study was so sprawling that the latitude and longitude varied enough intra-city to justify including these variables. Additionally, the random effect of the city variable accounts for spatial variation, which would render the inclusion of latitude and longitude redundant in the analysis. Model 5 is the same as model 4 but without city as a random effect. As expected, the fit on this model was not as good due to the violation of independence (related to Simpson's paradox).

Results

The mixed linear effects model tested to see if HOLC grade and Elevation (DEM) predicted the average land surface temperature of any given zone. The fitted model is as follows:

$$LST = \beta + 35.53\beta_1 + 1.29\beta_2 + 2.08\beta_3 + 2.30\beta_4 + -0.01\beta_5$$

Where β is our intercept that varies based on city, $\beta_{1\text{-}4}$ is HOLC Grades A-D, respectively, and β_5 is DEM. All *p* values are less than 0.001 and highly significant. The Conditional R^2 value (0.849) accounts for total variance explained through both the fixed and random effects, unlike the Marginal R^2 (0.374) which only accounts for the fixed effects (Nakagawa, 2013). As the inclusion of the random effects is vital to interpreting the results of this model, the conditional R^2 is the preferred metric between the two.

	MeanC		
Predictors	*Estimates*	*CI*	*p*
(Intercept)	35.53	34.86 – 36.20	**<0.001**
HOLC Grade [B]	1.29	1.14 – 1.44	**<0.001**
HOLC Grade [C]	2.08	1.93 – 2.22	**<0.001**
HOLC Grade [D]	2.30	2.14 – 2.45	**<0.001**
DEM mean	-0.01	-0.01 – -0.01	**<0.001**
Random Effects			
σ^2	4.08		
$\tau_{00\ CitySt}$	19.69		
ICC	0.83		
N_{CitySt}	202		
Observations	8844		
Marginal R^2 / Conditional R^2	0.374 / 0.849		

Table 3: Results of the linear mixed effects model

To test for multicollinearity in the model, the variance inflation factor (VIF) was calculated. Generally, a VIF value of 1 indicated no multicollinearity, and the higher the value, the more multicollinearity is present in the model. The VIF, equation shown below, for both DEM and HOLC grades was 1.033, indicating that there is little to no multicollinearity in the model.

$$VIF = \frac{1}{1 - R_1^2}$$

The residuals of the model are plotted below in figure 3 and appear randomly distributed. There are few outliers in the dataset of 8,844 samples, and none of them are extreme enough to be indicative of an underlying issue with the analysis. In the plotted residuals, there is a distinct break around 45°C. LST values have been recorded up to 58°C, but as these are extremes in the United States, values would be expected to level off well below that (Wan, 2006). Table II of the appendix lists all cities that have values over 45°C.

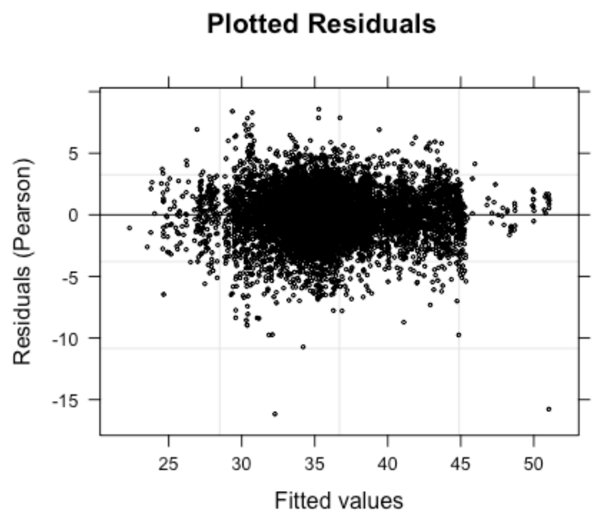

Figure 3: Plotted residuals of the chosen model

The residual outlier in the bottom right corner is zone 8476 in Phoenix, AZ that is ranked B and has a temperature of 50.6°C. Our model shows that B ranked zones are typically cooler than C or D ranks, but as Phoenix has 24 of its 25 zones at temperatures over 45°C, this zone is an anomaly even in the fitted values, but not indicative of errors in the dataset. Similarly, the other anomaly that has a residual value of roughly -15 is a D ranked zone in Seattle, WA that was recorded at only 16.1°C. Even with the fitted values of our model accounting for the variation between cities, the value is lower than expected. Due to the climate of Seattle, WA, this does not indicate unreliable values in our underlying dataset.

Discussion

The data suggest that there is a significant difference in temperature among HOLC grades, where the lowest ranked zones are the hottest. The figure and table below depict the estimated mean of each grade and the relationships among each rank. All grades are significantly different from each other (p<0.001). The largest difference in mean temperature is between zones ranked A and D. The results indicated that zones ranked D are an estimated 2.3°C hotter than zones ranked A. This is in line with the hypothesis of this study that historically redlined zones are on average hotter than their non-redlined zones within each city.

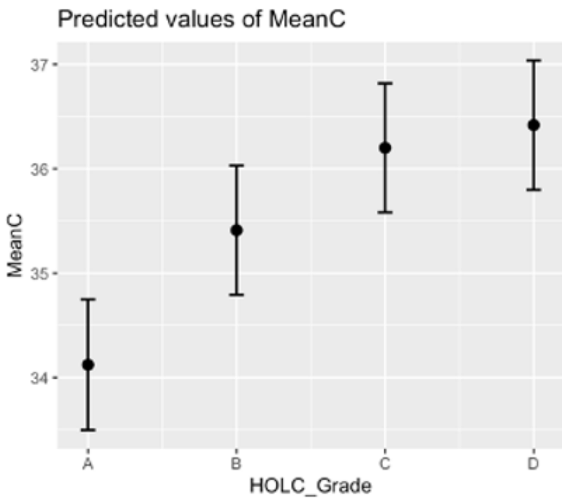

Contrast	Estimate	SE	*p*-value
A - B	-1.288	0.077	<0.0001
A - C	-2.077	0.074	<0.0001
A - D	-2.295	0.080	<0.0001
B - C	-0.789	0.056	<0.0001
B - D	-1.007	0.063	<0.0001
C - D	-0.218	0.057	0.0008

Table 4: The estimated difference among all zones, the significance, and standard error.
Figure 4: The estimated marginal means, or least squared means, of each HOLC grade.

Segregated neighborhoods existed long before and after the HOLC and its infamous maps. Redlining maps were not the origin of segregated housing, but instead were descriptions of practices already occurring in cities. Non-white and lower-class residents were often restricted to areas that were less desirable due to their proximity to pre-existing environmental detriments such as landfills and flood plains (Mizutani, 2018). Along with built infrastructure such as highways, these environmental factors were used as natural dividers of different zones to prevent the "infiltration of inharmonious racial groups" as referred to in the FHA's *Underwriting Manual*. Since the Fair Housing Act of 1968, discriminatory practices in the housing market have been declared illegal. Despite the law, a 2005 study found that "the dual market structure of the current mortgage industry… still denies lower-income minorities equal access to prime mortgages" (Apgar et al., 2005). Underinvestment in lower-class neighborhoods combined with discriminatory mortgage lending practices in the present day solidify the pattern of built environments and deprive residents of the means to build wealth through real estate.

Without investment in such neighborhoods, historically redlined zones will continue to have less access to green spaces (Nardone et al., 2021) that can dissipate heat more efficiently than impervious surfaces.

Other detriments to the desirability of land in the redlining guides included landfills, factories, and transportation infrastructure. These factors are high contributors to pollution and living in proximity increases one's exposure to dangerous contaminants (Mor et al., 2006; Liu et al., 2014). As a result, many of the C and D ranked zones experience higher levels of pollution and an increased risk of pollution-related illnesses (Nardone et al., 2020a; Nardone et al., 2020b; Beyer et al., 2016). Poor air quality is intensified by the UHI effect (Lai et al., 2009), and has been linked to asthma (Neidel, 2004) and cancer (Singer, 2011). Cognitive function has also been shown to decline in extreme heat (Gaoua, 2010; Taylor et al., 2016). The results of this study imply that zones ranked C and D are hotter than zones ranked A and B and are therefore exposed to intensified health risks.

Because factors such as health, race, class, heat exposure, and so on are interconnected, it is likely impossible to determine causality. Additionally, the inclusion of multiple social variables in linear models introduces multicollinearity and reduces reliability of results. Future studies could incorporate social data such as age, race, and class using a principal components analysis to explore deeper connections between the historic redlined zones and the neighborhoods they comprise in the present day.

Conclusion

While all cities that were subject to historic redlining experience the urban heat island effect, certain zones within the city that were ranked C or D by the HOLC experience even higher temperatures than zones ranked A or B. Through this analysis of 202 cities, the average LST of D ranked zones was 2.3°C higher than that of A ranked zones. These findings indicate that despite the cessation of overt race-based housing policies, the effects of such policies are socially and environmentally measurable in the present day. Without investment in these communities to increase greenspace, this trend will continue.

Literature Cited

Apgar, William C., and Allegra Calder. "The dual mortgage market: The persistence of discrimination in mortgage lending." (2005): 101.

Baston, Daniel (2021). *exactextractr: Fast Extraction from Raster Datasets using Polygons*. https://isciences.gitlab.io/exactextractr/, https://github.com/isciences/exactextractr.

Benmarhnia, Tarik, et al. "Comparing Urban and Rural Vulnerability to Heat-Related Mortality: A Systematic Review and Meta-Analysis." *Journal of Global Epidemiology and Environmental Health*, 2017, pp. 9–15, https://doi.org/10.29199/geeh.101016.

Beyer, Kirsten MM, et al. "New spatially continuous indices of redlining and racial bias in mortgage lending: links to survival after breast cancer diagnosis and implications for health disparities research." *Health & Place* 40 (2016): 34-43.

Bullard, Robert Doyle, Glenn Steve Johnson, and Angel O. Torres, eds. *Highway robbery: Transportation racism & new routes to equity*. South End Press, 2004.

Ermida, Sofia L. et al. "Google Earth Engine Open-Source Code for Land Surface Temperature Estimation from the Landsat Series." Remote Sensing 12.9 (2020): 1471.

Federal Housing Administration. *Underwriting Manual, Underwriting and Valuation Procedure under Title 2 of National Housing Act (1936). Congressional Document*.

Gaoua, Nadia. "Cognitive function in hot environments: a question of methodology." *Scandinavian journal of medicine & science in sports* 20 (2010): 60-70.

Good, EJ, Ghent, DJ, Bulgin, CE, et al. (2017) A spatiotemporal analysis of the relationship between near-surface air temperature and satellite land surface temperatures using 17 years of data from the ATSR series. Journal of Geophysical Research: Atmospheres 122(17): 9185–9210.

Hanson, Andrew, et al. "Discrimination in mortgage lending: Evidence from a correspondence experiment." *Journal of Urban Economics* 92 (2016): 48-65.

Harlan, Sharon, et al. "Neighborhood microclimates and vulnerability to heat stress." *Social Science & Medicine*, Volume 63, Issue 11, 2006, pp. 2847-2863, https://doi.org/10.1016/j.socscimed.2006.07.030.

Hijmans, R. J., and J. van Etten. "Raster: geographic data analysis and modeling. R package." (2015).

Hillier, Amy E. “Redlining and the Home Owners’ Loan Corporation.” Journal of Urban History, vol. 29, no. 4, USA: SAGE Publications, pp. 394–420, doi:10.1177/0096144203029004002.

Liu, Guannan, et al. "An ecological risk assessment of heavy metal pollution of the agricultural ecosystem near a lead-acid battery factory." *Ecological indicators* 47 (2014): 210-218.

Mitchell, Bruce, and Juan Franco. “Holc ‘Redlining’ Maps: The Persistent Structure of Segregation and Economic Inequality " NCRC.” *NCRC*, National Community Reinvestment Coalition, 20 Mar. 2018, https://ncrc.org/holc/.

Mizutani, Julia. "In the backyard of segregated neighborhoods: An environmental justice case study of Louisiana." *Geo. Envtl. L. Rev.* 31 (2018): 363.

Mor, Suman, et al. "Leachate characterization and assessment of groundwater pollution near municipal solid waste landfill site." *Environmental monitoring and assessment* 118.1 (2006): 435-456.

Nakagawa, S. and Schielzeth, H. (2013), A general and simple method for obtaining R^2 from generalized linear mixed-effects models. Methods Ecol Evol, 4: 133-142. https://doi.org/10.1111/j.2041-210x.2012.00261.x

Nardone, Anthony, et al. "Associations between historical residential redlining and current age-adjusted rates of emergency department visits due to asthma across eight cities in California: an ecological study." *The Lancet Planetary Health* 4.1 (2020): e24-e31.

Nardone, Anthony, Joey Chiang, and Jason Corburn. "Historic redlining and urban health today in US cities." *Environmental Justice* 13.4 (2020): 109-119.

Neidell, Matthew J. "Air pollution, health, and socio-economic status: the effect of outdoor air quality on childhood asthma." *Journal of health economics* 23.6 (2004): 1209-1236.

Nardone, Anthony, et al. "Redlines and greenspace: The relationship between historical redlining and 2010 greenspace across the United States." *Environmental health perspectives* 129.1 (2021): 017006.

Pebesma, Edzer (2018). “Simple Features for R: Standardized Support for Spatial Vector Data.” *The R Journal*, **10**(1), 439–446. doi: 10.32614/RJ-2018-009, https://doi.org/10.32614/RJ-2018-009.

Rothstein, Richard. *The Color of Law: A Forgotten History of How Our Government Segregated America*. Liveright Publishing Corporation, a Division of W.W. Norton & Company, 2018.

Sheffield, Perry, et al. “Not so little differences: variation in hot weather risk to young children in New York City.” *Public Health,* 2018, pp.119-126, https://doi.org/10.1016/j.puhe.2018.06.004.

Singer, Merrill. "Down cancer alley: The lived experience of health and environmental suffering in Louisiana's chemical corridor." *Medical Anthropology Quarterly* 25.2 (2011): 141-163.

Stafoggia, Massimo, et al. “Vulnerability to Heat-Related Mortality: A Multicity, Population-Based, Case-Crossover Analysis.” *Epidemiology*, vol. 17, no. 3, Lippincott Williams & Wilkins, 2006, pp. 315–23, http://www.jstor.org/stable/20486220.

Susca, T, S.R. Gaffin, G.R. Dell’Osso, Positive effects of vegetation: Urban heat island and green roofs, Environmental Pollution, Volume 159, Issues 8–9, 2011, Pages 2119-2126, ISSN 0269-7491, https://doi.org/10.1016/j.envpol.2011.03.007.

Taylor, Lee, et al. "The impact of different environmental conditions on cognitive function: a focused review." *Frontiers in physiology* 6 (2016): 372.

Wan, Zhengming. "MODIS land surface temperature products users’ guide." *Institute for Computational Earth System Science, University of California: Santa Barbara, CA, USA* 805 (2006).

Appendix

Grade	Count	Area (km^2)
A	1039	1271.69
B	2327	2679.82
C	3381	5185.00
D	2118	3282.71

Table I: Nationwide Count of HOLC zones and total area

List of cities included in this study:

Alabama: Birmingham, Mobile, Montgomery
Arizona: Phoenix
Arkansas: Little Rock
California: Fresno, San Diego, San Francisco, San Jose, Stockton, Sacramento, Oakland, Los Angeles
Colorado: Denver, Pueblo
Connecticut: New Haven, Stamford, Darien, New Canaan, New Britain, Hartford, Waterbury
Florida: Miami, Jacksonville, St. Petersburg, Tampa
Georgia: Atlanta, Augusta, Columbus, Macon, Savannah
Illinois: Aurora, Chicago, Rockford, Joliet, Springfield, East St. Louis, Decatur, Peoria
Indiana: Muncie, Evansville, Fort Wayne, Lake Co. Gary, Terre Haute, South Bend, Indianapolis
Iowa: Waterloo, Sioux City, Des Moines, Davenport, Council Bluffs, Dubuque
Kansas: Wichita, Topeka
Kentucky: Louisville, Lexington, Covington
Louisiana: New Orleans, Shreveport
Maryland: Baltimore
Massachusetts: Boston, Milton, Dedham, Quincy, Braintree, Brookline, Winthrop, Needham, Newton, Watertown, Waltham, Cambridge, Somerville, Medford, Malden, Arlington, Belmont, Lexington, Winchester, Everett, Melrose, Revere, Chelsea, Saugus, Haverhill, Holyoke Chicopee, Brockton
Michigan: Kalamazoo, Battle Creek, Bay City, Flint, Grand Rapids, Muskegon, Pontiac, Detroit, Saginaw, Lansing, Jackson
Minnesota: Duluth, St. Pail, Rochester, Minneapolis
Mississippi: Jackson
Missouri: St. Joseph, Springfield, Greater Kansas City, St. Louis
Nebraska: Omaha, Lincoln
New Hampshire: Manchester
New Jersey: Hudson Co., Atlantic City, Camden, Essex Co., Bergen Co., Trenton, Union Co.

New York: Utica, Troy, Rochester, Queens, Poughkeepsie, Manhattan, Brooklyn, Bronx, Staten Island, Schenectady, Syracuse, Albany, Elmira, Binghamton-Johnson City, Niagara Falls, Lower Westchester Co., Buffalo
North Carolina: Asheville, Charlotte, Durham, Greensboro, Winston-Salem
Ohio: Youngstown, Hamilton, Warren, Cleveland, Columbus, Portsmouth, Toledo, Lorain, Lima, Dayton, Springfield, Akron, Canton
Oklahoma: Tulsa, Oklahoma City
Oregon: Portland
Pennsylvania: Pittsburgh, New Castle, Altoona, Philadelphia, Johnstown, Erie, Harrisburg, Lancaster, Bethlehem, Chester, Wilkes-Barre, York
Rhode Island: Providence, Woonsocket, Pawtucket, Central Falls
South Carolina: Columbia
Tennessee: Knoxville, Chattanooga, Nashville, Memphis
Texas: Dallas Houston, San Antonio, Amarillo, Beaumont, El Paso, Fort Worth, Galveston, Waco, Austin, Port Arthur
Utah: Salt Lake City, Ogden
Virginia: Richmond, Roanoke, Norfolk, Newport News, Lynchburg
Washington: Seattle, Spokane, Tacoma
Wisconsin: Kenosha, Madison, Oshkosh, Racine, Milwaukee Co.
West Virginia: Charleston, Wheeling, Huntington

City	Count of zones over 45°C	Total number of zones by city
Los Angeles, CA	152	416
San Diego, CA	26	76
Phoenix, AZ	24	25
El Paso, TX	23	23
Oklahoma City, OK	11	90
Fresno, CA	10	24
Ogden, UT	3	23
Miami, FL	1	74
Lincoln, NE	1	22
Salt Lake City, UT	1	29

Table II: Cities with zones over 45°C

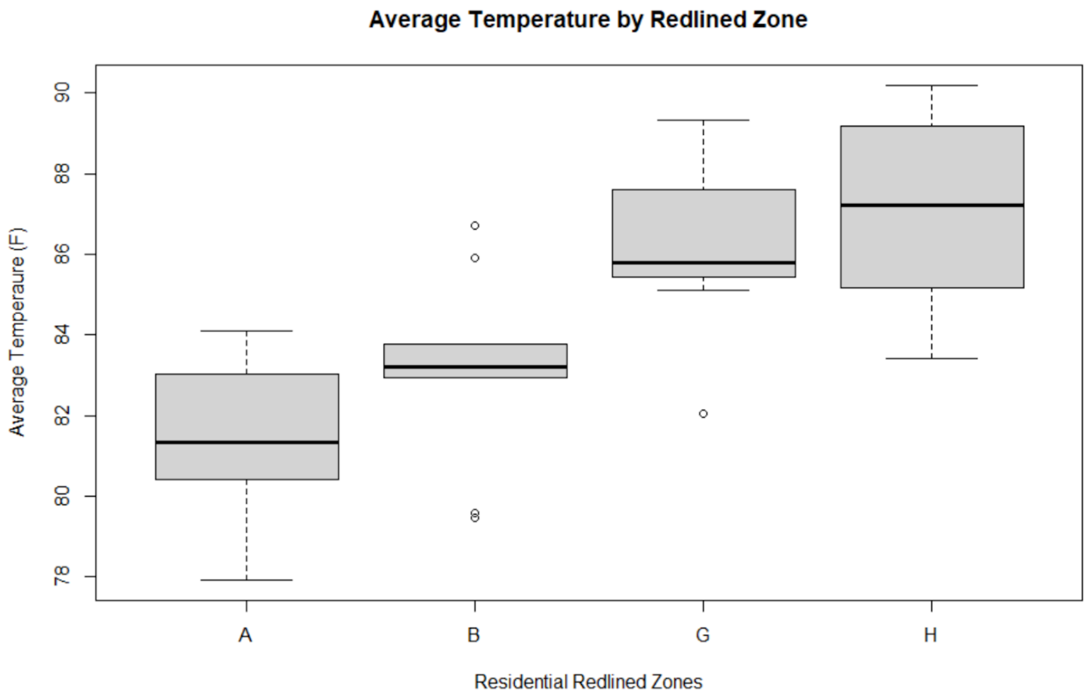

Figure I: Boxplot showing temperature differences in the sample D.C. tests. D.C. was omitted from this study due to a different ranking system, where A and B were still the highest ranks, but G and H correspond with the HOLC's rating of C and D. There were additional rankings (C-F) that designated various other classifications such as nonresidential. An ANOVA test was performed comparing the average LST of rankings A, B, G, and H. Both highest ranked zones (A and B) were significantly different ($p<0.05$) than the two lowest ranked zones (G and H). Specifically, the analysis showed that the areas of the city that were once classified as H are now on average 3.1°C hotter than areas that were classified as A.